



Physiology regulates the relationship between coccosphere geometry and growth-phase in coccolithophores

Rosie M. Sheward^{1,2}, Alex J. Poulton³, Samantha J. Gibbs¹, Chris J. Daniels³, Paul R. Bown⁴

¹ Ocean and Earth Science, University of Southampton, National Oceanography Centre, Southampton, SO14 3ZH, United Kingdom.

² Institute of Geosciences, Goethe-University Frankfurt, 60438 Frankfurt am Main, Germany.

³ Ocean Biogeochemistry and Ecosystems, National Oceanography Centre, Southampton, SO14 3ZH, United Kingdom.

⁴ Department of Earth Sciences, University College London, Gower Street, London, WC1E 6BT, United Kingdom.

10 Correspondence to: Rosie M. Sheward (sheward@em.uni-frankfurt.de)

Abstract. Coccolithophores are an abundant phytoplankton group that exhibit remarkable diversity in their biology, ecology, and calcitic exoskeletons (coccospheres). Their extensive fossil record is testament to their important biogeochemical role and is a valuable archive of biotic responses to environmental change stretching back over 200 million years. However, to realise the potential of this archive requires an understanding of the physiological processes that underpin coccosphere architecture. Using culturing experiments on four modern coccolithophore species (*Calcidiscus leptoporus*, *Calcidiscus quadriperforatus*, *Helicosphaera carteri* and *Coccolithus braarudii*) from three long-lived families, we investigate how coccosphere architecture responds to shifts from exponential (rapid cell division) to stationary (slowed cell division) growth phases as cell physiology reacts to nutrient depletion. These experiments reveal statistical differences in cell size and the number of coccoliths per cell between these two growth phases, specifically that cells in exponential-phase growth are typically smaller with fewer coccoliths, whereas cells experiencing growth-limiting nutrient depletion have larger coccosphere sizes and greater numbers of coccoliths per cell. Although the exact numbers are species-specific, these growth-phase shifts in coccosphere geometry demonstrate that the core physiological responses of cells to nutrient depletion results in increased cell sizes and coccoliths per cell across four different coccolithophore families (Calcidiscaceae, Coccolithaceae, Isochrysidaceae, Helicosphaeraceae), a representative diversity of this phytoplankton group. Building on this, direct comparison of coccosphere geometries in modern and fossil coccolithophores enables a proxy for growth phase to be developed that allows growth responses to environmental change to be investigated throughout their evolutionary history. Our data also shows that changes in growth rate and coccoliths per cell associated with growth-phase shifts can substantially alter cellular calcite production. Coccosphere geometry is therefore a valuable tool for accessing growth information in the fossil record that provides unprecedented insights into the biotic responses of species to environmental change and its potential biogeochemical consequences.



1 Introduction

The fossil remains of biomineralised plankton provide comprehensive records of their biogeography, ecology, diversity and evolution that have significance for our understanding of past ocean and climate systems and its influence on these microscopic organisms. Despite their small size ($\sim < 63 \mu\text{m}$), the vast numbers of photosynthesising plankton in the ocean drive many regional- to global-scale biogeochemical processes and comprise the biomass that sustains the wider diversity of marine life at higher trophic levels (e.g., Menden-Deuer and Kiørboe, 2016). Investigating the biological response of plankton species to environmental variability is therefore a crucial step in understanding the potential consequences of future climate change on marine systems.

Coccolithophores are a major group of calcifying marine algae that first evolved more than 200 million years ago (Ma) during the Late Triassic (Janofske, 1992; Bown et al., 2004). The remains of their calcite cell coverings contribute to the export of biogenic carbonate to deep-sea sediments (Broecker and Clark, 2009), forming a geographically and temporally extensive fossil record that is mostly in the form of individual calcite plates called coccoliths. Spatial and temporal analysis of coccoliths reveals the evolution, biogeography and ecology of past species (e.g., Haq and Lohmann, 1976; Knappertsbusch, 2000; Ziveri et al., 2004; Gibbs et al., 2006; Baumann et al., 2016) and the response of species and communities to palaeoceanographic and palaeoclimatic variability (e.g., Bollmann et al., 2002; Bown, 2005; Bollmann et al., 2009; Bown and Pearson, 2009).

Valuable new insights into past coccolithophore communities can also be provided by the study of intact fossil coccospheres that have not disarticulated into their component coccoliths, providing intriguing snapshots of individual cell growth in geological time (Gibbs et al., 2013; Bown et al., 2014; O'Dea et al., 2014). The discovery of relatively abundant fossil coccospheres in exceptionally well-preserved sedimentary deposits inspired Gibbs et al. (2013) to first explore the quantitative links between coccosphere geometry (coccosphere size, coccolith length and coccolith number) and population growth. Their laboratory experiments using the modern species *Coccolithus braarudii* and *Emiliana huxleyi* identified that cells undergoing rapid cell division (termed 'exponential-phase' growth) were smaller and had fewer coccoliths per coccosphere compared to cells dividing slowly, or not at all ('stationary-phase' growth). This initial evidence for a relationship between growth phase and coccosphere geometry was then used to reconstruct the response of fossil taxa (*Coccolithus* and *Toweius*) through an interval of rapid warming ~ 56 Ma called the Paleocene-Eocene Thermal Maximum (Gibbs et al., 2013; O'Dea et al., 2014). As growth phases describe 'states' of rapid or slowed growth rates, these findings hint that coccosphere geometry could provide new insights into the fitness and subsequent evolutionary success of coccolithophore populations where growth rates (or other measures of fitness) cannot be measured directly.

The development of coccosphere geometry as an indicator, or even proxy, of growth phase in the fossil record requires further evidence that phases of rapid and slowed growth produce quantifiably distinct differences in coccosphere geometry, which can be regarded as a 'universal' feature of coccolithophores rather than just a species-specific attribute. Even across the diversity of modern species, we observe substantial variability in cell size, coccolith length and numbers of



coccoliths per cell. Given this observation, can we reasonably hypothesise that the growth-geometry relationship reported by Gibbs et al. (2013) for two modern species is similar across coccolithophores in general? If this is the case, then coccosphere geometry could prove to be a valuable proxy for growth phase, and hence overall population fitness. One potential concern is that coccolithophores show pronounced species-specific and even strain-specific physiological responses to a variety of environmental manipulations such as carbonate chemistry and nutrient availability in culture experiments (Langer et al., 2006; Langer et al., 2009; Krug et al., 2011), which may extend to coccosphere variability. We therefore require coccosphere geometry data from multiple modern species experiencing different growth phases in order to further investigate the relationship between coccosphere geometry and growth.

Here, we aimed to determine relationships (if any) between growth phase and coccosphere geometry in three modern coccolithophore species – *Calcidiscus leptoporus*, *Calcidiscus quadriperforatus* and *Helicosphaera carteri* - and to integrate these new data with those previously determined by Gibbs et al. (2013) for *Coccolithus* and *Emiliania*. *Calcidiscus* and *Helicosphaera* are particularly pertinent study taxa, as they have widespread modern and geological occurrences and are important components of mid- to low-latitude coccolithophore communities, preferring warmer temperate to tropical waters (Ziveri et al., 2004). These species are also three of the largest and most heavily calcified of all the modern species, along with *Coccolithus pelagicus* in the high latitudes and *Coccolithus braarudii* in the mid- to high-latitudes (Ziveri et al., 2004), and are therefore important contributors to the production (Daniels et al., 2014; Daniels et al., 2016) and export of inorganic carbon to the deep ocean (Ziveri et al., 2007). Variability in coccosphere geometry in these species, particularly the number of coccoliths per cell, could therefore substantially alter cellular calcite with significant consequences for calcite production and export. The well-documented fossil records of these genera extend back to the first occurrence of *Calcidiscus* ~57 Ma (Bown et al., 2007) and *Helicosphaera* ~54 Ma (Perch-Nielsen, 1985). Alongside *Coccolithus* they have been significant components of coccolithophore communities over much of the last ~55 Ma (Perch-Nielsen, 1985; Bown et al., 2007).

Helicosphaera and *Calcidiscus* also have distinct evolutionary and physiological differences that may highlight restriction of the growth-geometry relationship to specific lineages. Species within the Helicosphaeraceae (Order Zygodiscales) have evolved in a lineage quite separate to the Coccolithaceae and Calcidiscaceae (Order Coccolithales), with the two orders diverging very early in coccolithophore evolutionary history during the Jurassic, ~150-200 Ma (de Vargas et al., 2007). *Helicosphaera carteri* is also physiologically distinct from both *Coccolithus* and *Calcidiscus* species as it is motile in the diploid (heterococcolith-bearing) life-cycle phase. As the genera *Coccolithus* and *Calcidiscus* are considered to be relatively closely related but are still classified in separate families, we would predict that the growth-phase diagnostic features of coccosphere geometry in *Calcidiscus* species might be more likely to show fundamental similarities to those reported for *Coccolithus* by Gibbs et al. (2013). To our knowledge, the experiments undertaken for this study have produced the most extensive dataset of modern coccosphere geometry yet to be presented, comprising a total of more than 13,300 measurements of coccosphere and cell size, coccolith length and coccoliths per cell from 2,850 individual cells.



2 Methods

2.1 Experiment design

Monoclonal cultures of South Atlantic Ocean *Calcidiscus quadriperforatus* strain RCC 1135, *Calcidiscus leptoporus* strain RCC 1130 and *Helicosphaera carteri* strain RCC 1323 were obtained from the Roscoff Culture Collection (RCC) and maintained at an incubation temperature of 19 °C at the National Oceanography Centre, Southampton. Cultures were acclimated to new experimental temperature and light conditions for a minimum of two weeks (>10 generations) prior to the start of each experiment. The light regime remained consistent across all experiments at irradiance levels of 75 - 90 $\mu\text{mol photons m}^{-2} \text{s}^{-1}$ (equivalent to a daily photon flux of $\sim 7 \text{ mol photons m}^{-2} \text{d}^{-1}$) with a 12-hour light, 12-hour dark irradiance cycle. To achieve a range of cell division rates, experiments were undertaken at 16, 18, 20 and 22 °C, which is within the natural temperature range experienced by field populations of these three species (Ziveri et al., 2004).

For each temperature experiment, all three species were cultured simultaneously and in duplicate following a 'batch culture' procedure, where an initially low number of cells ml^{-1} are left to increase in density, using up nutrients, until initial nutrient levels are completely depleted and population growth ceases. This approach enables coccosphere geometry data to be collected from both nutrient-replete rapid cell-division days and nutrient-deplete slowed cell-division days towards the end of the experiment, as used successfully in the experiments of Gibbs et al. (2013) for *Coccolithus*. The initial starting density of cells for each experiment was $\sim 300 \text{ cells ml}^{-1}$ (taken from acclimated cultures) added to 350 ml of sterilised and filtered natural seawater with added nutrients (lower-nutrient K/20 medium, modified from Keller et al., 1987, following Langer et al., 2006; Gerecht et al., 2014 and Daniels et al., 2014). Lower-nutrient media was specifically used to ensure that cultures reached nutrient-limiting conditions before the occurrence of significant changes in carbonate chemistry (Daniels et al., 2014). The effect of increasing cell density on the carbonate chemistry of the media over the duration of the experiment was further minimised by using 650 ml polycarbonate flasks (Thermo Fisher Scientific) with vented lids to allow gas exchange between the culture media and the atmosphere outside the flask. After initial inoculation of the media, experiment cultures increase in cell number rapidly, termed the exponential growth phase, and were allowed to grow into stationary phase, at which point increasing nutrient limitation reduces growth rates such that the day-to-day increase in cells ml^{-1} decreases towards zero. The typical experiment duration between initial inoculation and the onset of stationary phase growth was 14-21 days.

2.2 Growth rate calculation

Daily cell abundance was determined from triplicate counts of cells ml^{-1} using a Sedgwick Rafter Cell (Pyser-SGI; following Langer et al., 2006) on a transmitted light microscope at x100 magnification. As *H. carteri* is a motile species, 40 μl per ml (4% final volume) 10% formaldehyde was added to the samples to inhibit movement prior to counting to ensure accuracy. Daily growth rates were calculated as the natural log of the difference in cell density between the census day and the day



before (Langer et al., 2006). The duration of the exponential growth phase was then determined by visual examination of
 130 these daily growth rates and plots of cell abundance over time.

2.3 Coccosphere geometry

Samples for light microscope (LM) analysis were taken daily using 2-5 ml of each culture replicate, filtered onto cellulose
 nitrate filters (pore size 0.8 µm; Sartorius Stedim Biotech) and dried overnight at 50 °C. One half of each filter was then
 fixed between a glass microscope slide and a cover slip using Norland Optical Adhesive 74 (Norland Products Inc.) and
 135 cured under UV light exposure. The other half of each filter was stored for future scanning electron microscope (SEM)
 analysis or for additional replicate LM slides if needed. All LM analysis was performed using a cross-polarised light
 microscope (Olympus BX51) with a colour camera attached (Olympus DP71). Coccosphere geometry data was obtained
 through LM following the same techniques applied by Gibbs et al. (2013) and Daniels et al. (2014), and described in detail
 here. Random transects across the widest section of the filter hemisphere were performed until 30 individual coccospheres
 140 per slide were located from slides corresponding to alternate day or, in some instances, daily samples. First, the number of
 coccoliths around each cell (C_N) was counted by finely adjusting focal depth. Then, in-focus images of the upper
 coccosphere surface and maximum cell cross-section were captured from which biometric measurements (Fig. 1) of
 coccolith length (C_L), coccosphere size (\emptyset ; size including calcite covering) and cell size (Θ ; size excluding calcite covering)
 were taken (Cell[^]D software, Olympus). Unlike the spherical coccospheres of *Coccolithus* and *Calcidiscus* species, *H.*
 145 *carteri* coccospheres are prolate spheroids (Fig. 4), so here we report cell and coccosphere sizes for this species as equivalent
 spherical diameters. Prolate spheroid volume is calculated as $V = (\pi/6)d^2h$, where d is the short-axis cell/coccosphere
 diameter and h is the long-axis cell/coccosphere height (Sun and Liu, 2003). This volume is used to calculate equivalent
 spherical radius. This coccosphere geometry dataset is available from <https://doi.pangaea.de/10.1594/PANGAEA.865403>,
 doi registration in progress.

150 2.4 Cellular calcite calculation

Particulate inorganic carbon (PIC) per cell was calculated following Young and Ziveri (2000):

$$\text{Cellular PIC (pmol C cell}^{-1}\text{)} = \frac{C_N \times C_L^3 \times k_s \times 2.7}{100} \quad (1)$$

where C_N is number of coccoliths per cell, C_L is coccolith length (µm), k_s is a shape factor that numerically describes
 species-specific coccolith morphology, and 2.7 pg µm⁻³ is the density of calcite. Division by 100 calculates cellular PIC in
 155 pmol C cell⁻¹ from pg cell⁻¹. We use the shape factors of $k_s = 0.08$ for *Calcidiscus* spp., $k_s = 0.05$ for *H. carteri*, and $k_s = 0.06$
 for *Coccolithus* spp. from Young and Ziveri (2000).



2.5 Additional experimental results from *Coccolithus*

This study reports the new experimental results for *Calcidiscus* and *Helicosphaera* alongside coccosphere geometry and growth data for *Coccolithus* from two previous studies that used identical LM methods to collect coccosphere geometry data.

- 160 Gibbs et al. (2013) obtained coccosphere geometry data from a comparable batch culture experiment at a single temperature in *Coccolithus braarudii* strain RCC 1197. This data is presented for direct comparison with the three new species of this study, as much of the Gibbs et al. (2013) data was originally presented as Supplementary Information to accompany that short-format paper. We also present results from a previously unanalysed dataset of exponential-phase coccosphere geometry in *C. braarudii* strain RCC 1198 and *C. pelagicus* strain RCC 4092, originally published as a data report by
 165 Sheward et al. (2014) and available from <http://www.pangaea.de> (doi: 10.1594/PANGAEA.836841). For that study, batch culture experiments were undertaken at multiple temperatures (6–12 °C in *C. pelagicus* and 12–19 °C in *C. braarudii*) and samples for coccosphere geometry analysis collected on a single mid-exponential phase experiment day (further details in Daniels et al., 2014).

3. Results

170 3.1 Growth rates

The four temperature experiments resulted in a modest range of daily and mean exponential growth rates (μ) across *Helicosphaera* and *Calcidiscus* species. The highest exponential growth rate for *C. quadriperforatus* was achieved at 22 °C ($\mu = 0.44 \text{ d}^{-1}$), for *C. leptoporus* at 20 °C ($\mu = 0.44 \text{ d}^{-1}$), and for *H. carteri* at 20 °C ($\mu = 0.45 \text{ d}^{-1}$). Mean exponential growth rates for *C. braarudii* at 15 °C were 0.68 d^{-1} . These values are well within the ranges reported in other studies carried out at
 175 similar temperatures for *Calcidiscus* (Langer et al., 2006; Buitenhuis et al., 2008; Fiorini et al., 2010; 2011; Langer et al., 2012; Candelier et al., 2013; Müller et al., 2014) and *H. carteri* (Stoll et al., 2002; Šupraha et al., 2015). Exponential growth rates of $0.4\text{--}0.5 \text{ d}^{-1}$ signify that roughly half of the culture population undergoes cell division each day. Maximum cell density was $\sim 100,000 \text{ cells ml}^{-1}$ in *C. leptoporus* cultures, $60\text{--}100,000 \text{ cells ml}^{-1}$ for *C. quadriperforatus*, $\sim 30,000 \text{ cells ml}^{-1}$ for *H. carteri* and $\sim 25,000 \text{ cells ml}^{-1}$ for *C. braarudii*.

180 3.2 Within-species range in coccosphere geometry

Coccosphere (\emptyset) and cell size (Θ), coccolith length (C_L) and number of coccoliths per cell (C_N) show clear species-specific differences (Fig. 2, Table 1). A considerable range in \emptyset is seen in all species; $15 \mu\text{m}$ to $25 \mu\text{m}$ in *C. quadriperforatus*, and $10 \mu\text{m}$ to $15 \mu\text{m}$ in *H. carteri* and *C. leptoporus*. This is a comparable \emptyset range to *C. pelagicus* (12 to $22 \mu\text{m}$) but slightly less than the \emptyset range observed in *C. braarudii* (15 to $30 \mu\text{m}$).

- 185 *Calcidiscus* spp. and *H. carteri* show a much greater range in C_N compared to *Coccolithus* spp. (Fig. 2e–h). The most frequently observed C_N is 16 in *H. carteri* cells, 18 in *C. quadriperforatus* cells, and 19 in *C. leptoporus* cells, with a



maximum number of ~30 coccoliths in all of these species. In contrast, *Coccolithus* cells more typically have 11-12 coccoliths per cell, up to a maximum of 20-23 coccoliths. In one *C. leptoporus* cell, the coccosphere was formed from 45 coccoliths (Fig. 4c). The relationship between C_N and \emptyset subsequently shows a steeper gradient in *Helicosphaera* and *Calcidiscus* (greater C_N increase per μm \emptyset) compared to *Coccolithus* (Fig. 2). The comparable coccosphere sizes but significantly greater number of coccoliths per coccosphere of *C. quadriperforatus* compared to *C. braarudii*, and *C. leptoporus* compared to *C. pelagicus*, suggests that *Calcidiscus* species achieve a greater degree of coccolith overlapping compared with *Coccolithus* species of a similar coccolith size. This is likely the result of the circular shape and narrower central tube structure in *Calcidiscus* coccoliths, which therefore pack more tightly around the cell with increasing C_N , moderating a corresponding increase in \emptyset . The minimum C_N in *H. carteri* is similar to *Coccolithus* ($C_N = 6$ and $C_N = 5-7$, respectively). The smallest cells, with just 6 coccoliths, observed in *H. carteri*, formed cuboid coccospheres (Fig. 4a) and are most likely recently-divided cells. Cubiform coccospheres have also been reported in Bown et al. (2014) for the extinct Paleogene taxa *Toweius pertusus* and *Umbilicosphaera bramlettei* and ‘boxy’ coccospheres are also seen in several *Chiasmolithus* species, which are probably also related to small cell sizes soon after cell division.

Although coccosphere geometry is similar in the two closely-related *Calcidiscus* species (Fig. 2f, g), it is not identical, with *C. leptoporus* producing coccospheres with a slightly greater C_N on average than *C. quadriperforatus*. In contrast, the two species of *Coccolithus* are closely comparable, with the linear regression gradient between \emptyset and C_N the same in both *C. pelagicus* and *C. braarudii*, although the gradients are offset from each other (Fig. 2h). Until recently, these two *Calcidiscus* species were considered to be intraspecific morphotypes (Knappertsbusch et al., 1997; Knappertsbusch, 2000) or sub-species (Geisen et al., 2002) but have since been shown to be genetically-distinct, which is also the case for *C. pelagicus* and *C. braarudii* (Saez et al., 2003; de Vargas et al., 2004). The considerable overlap in C_L , \emptyset and C_N in *Calcidiscus* species makes species-differentiation based solely on any one of these parameters difficult. However, the species-specific coccosphere geometry identified here lends further support to the genetic distinction between these species, alongside previously identified morphological and ecological differences (Knappertsbusch et al., 1997; Knappertsbusch, 2000; Geisen et al., 2002; Renaud et al., 2002; Saez et al., 2003; Geisen et al., 2004; Baumann et al., 2016).

Coccolith length varies between cells by up to 4.5 μm in *H. carteri*, 6.0 μm in *C. quadriperforatus*, and 3.7 μm in *C. leptoporus*, which is similar to C_L ranges between 3.0 to 8.5 μm reported in selected studies on sediment samples (e.g., Baumann, 2004; Henderiks and Törner, 2006; Herrmann et al., 2012; Baumann et al., 2016). Unfortunately, no culturing experiments on *Calcidiscus* or *Helicosphaera* report C_L measurements for comparison. In contrast to C_N , C_L shows no relationship with \emptyset within these clonal populations (Fig. 2i-l) and superimposing C_N onto plots of \emptyset against C_L (Fig. 2m-p) clearly demonstrates the strong co-variance of \emptyset and C_N . In our clonal populations, cell division is fully synchronised across cells resulting in relatively restricted ranges in \emptyset and C_L that have no statistically-significant relationship (Fig. 2i-l). A weak relationship between \emptyset and C_L appears to exist in *Coccolithus* when data for *C. pelagicus* is combined with data from two strains of *C. braarudii* (Fig. 2l, p). This C_L - \emptyset relationship only occurs in these culture experiments when data from several growth-synchronised populations are mixed, an effect illustrated in the culture and field data of Gibbs et al. (2013) that is



greatly amplified in fossil assemblages that typically integrate the remains of surface populations over long time-spans (Gibbs et al., 2013, their Fig. 3a). In our single-clone culture populations however, the principle coccosphere geometry relationship is between C_N and \emptyset rather than C_L and \emptyset .

3.3 Coccosphere geometry as a function of growth

225 This study demonstrates that coccosphere size in all species studied is statistically smaller during experiment days of rapid, nutrient-replete, exponential-phase growth than during days of slowed, nutrient-depleted, early stationary-phase growth (Fig. 3). Mean \emptyset across all four temperature experiments during exponential-phase growth is 14.8 μm in *H. carteri*, 18.4 μm in *C. quadriperforatus*, 13.1 μm in *C. leptoporus* and 20.5 μm in *C. braarudii*. Coccosphere diameter during non-exponential growth is modestly but statistically (unpaired t-test) larger than during exponential-phase growth, with mean \emptyset 0.55 μm larger in *C. quadriperforatus* ($t=3.324$, $df=839$, $p<0.001$) and *H. carteri* ($t=4.659$, $df=990$, $p<0.0001$), and 0.7 μm larger in *C. leptoporus* ($t=5.669$, $df=1020$, $p<0.0001$). Mean \emptyset in *C. braarudii* (Gibbs et al., 2013) shows a larger increase of 1.75 μm ($t=9.216$, $df=548$, $p<0.0001$) between exponential and early stationary growth. An increase in cell size has also previously been observed in response to nutrient limitation in *Coccolithus* and *Helicosphaera* (Gerecht et al., 2014; Gerecht et al., 2015; Šupraha et al., 2015).

235 In addition to size differences, coccospheres also typically consist of fewer coccoliths during exponential-phase growth and a greater number of coccoliths during early stationary-phase growth (Fig. 3). Cells no longer able to maintain exponential rates of growth have an average of 1-2 extra coccoliths per cell in *H. carteri* ($t=5.067$, $df=990$, $p<0.0001$) and *C. quadriperforatus* ($t=5.451$, $df=840$, $p<0.0001$), 2-3 extra coccoliths per cell in *C. leptoporus* ($t=6.312$, $df=1020$, $p<0.0001$) and 3-4 extra coccoliths per cell in *C. braarudii* ($t=14.24$, $df=548$, $p<0.0001$). The frequency distribution of C_N for each species (Fig. 3) can be used as a quantitative indicator of whether cells are in a recently-divided state (close to the minimum number of coccoliths per cell observed, $C_N \leq 10^{\text{th}}$ percentile of the data) or are in a ready-to-divide state (close to the maximum number of coccoliths per cell observed, $C_N \geq 90^{\text{th}}$ percentile of the data). These C_N ‘thresholds’ for recently-divided and ready-to-divide cells for each species are shown in Fig. 3 and Table 1. Based on the species-specific geometries observed, recently-divided cells typically have $C_N \leq 12$ in *H. carteri* and $C_N \leq 14$ in *Calcidiscus* spp., whilst cells that are ready to divide have $C_N \geq 21$ in *H. carteri*, $C_N \geq 23$ in *C. quadriperforatus*, and $C_N \geq 25$ in *C. leptoporus* (Fig. 3). During exponential growth, the C_N of the population is typically skewed towards the minimum observed C_N , whereas populations exhibiting slowed growth are more likely to have a greater number of cells in a ready-to-divide state.

4. Discussion

4.1 Physiological insights into coccosphere geometry

250 Within these experiments, coccosphere size (\emptyset) and the number of coccoliths per cell (C_N) varied depending on whether the culture population was increasing in cell numbers each day at a rapid rate (exponential-growth phase) or a slowed rate (non-



exponential-growth phase). Across all four species investigated, the transition from exponential into non-exponential phase growth was clearly associated with a shift towards an increased abundance of cells with a greater C_N and larger coccosphere sizes by $\sim 2 \mu\text{m}$ (Fig. 3), representing a statistically significant increase of 10-15% on exponential-phase size. C_N is not a frequently recorded variable but where $\bar{\Theta}$ and C_N in both nutrient-replete and nutrient-deplete cultures can be inferred from supplementary information (Balch et al., 1993; Paasche, 1998; Gerecht et al., 2014; Gerecht et al., 2015; Šupraha et al., 2015) these are consistent with the extensive observations from our experiments for *Calcidiscus* and *H. carteri* and in Gibbs et al. (2013) for *C. braarudii*.

The relationship between growth phase, $\bar{\Theta}$ and C_N can be understood by considering the process of cell division and how it is affected by the nutrient depletion that instigates non-exponential-phase growth. Both $\bar{\Theta}$ and C_N vary as each cell progresses through the cell division cycle (unpublished observations; Taylor et al., 2007; Müller et al., 2008). Cells that have recently undergone division are small with approximately the minimum number of coccoliths required to form a complete cell covering (unpublished observations; Fig. 4). After division, cells recommence coccolith production, which is shown in these experiments to increase C_N until the cell has sufficient coccoliths to cover two newly divided cells. Coccosphere diameter correspondingly increases alongside increasing C_N as the cell synthesises organic cellular components such as proteins, lipids and carbohydrates. Cultures that are able to maintain exponential rates of cell division subsequently have a lower mean $\bar{\Theta}$, $\bar{\Theta}$ and C_N as the majority of cells are in a ‘recently divided’ state (Fig. 3, 4). When cells are no longer able to maintain exponential rates of cell division, in this instance due to decreasing nutrient availability, they divide less frequently on average. This is observed in the later days of each experiment as an increase in the mean $\bar{\Theta}$, $\bar{\Theta}$ and C_N , an interpretation that is consistent with the findings of Gibbs et al. (2013).

An increase in cell size, $\bar{\Theta}$, under decreasing nutrient availability may seem counterintuitive, as nutrients are essential for phytoplankton growth. Nitrate and phosphate are the two key nutrients required by most phytoplankton (Arrigo, 2005; Moore et al., 2013) and they fulfil different purposes within the cell. Phosphate limitation primarily impedes production of the RNA, phospholipids and DNA that are essential for cell replication, and phosphate is a key component of cellular energy carriers (Zhao et al., 2015). Nitrate limitation particularly impacts the synthesis of proteins and pigments used in photosynthesis (Zhao et al., 2015). Nutrient limitation therefore suppresses cell division and growth in multiple ways. However, cell size and particulate organic carbon content (POC) have been consistently shown to increase under nutrient limited conditions (e.g., Müller et al., 2008) as the cell is still able to produce non-essential lipids and carbohydrates.

The greater C_N of coccospheres during non-exponential-phase growth (Fig. 3) includes the occurrence of some large coccospheres with very high C_N (Fig. 4) and more than enough coccoliths to cover two daughter cells. This is evidence that cellular calcification (coccolith production) can proceed uninterrupted despite decreasing nutrient availability and indicates that the calcification process has a lower nutrient ‘cost’ compared to cell division processes (Paasche, 1998; Monteiro et al., 2016). This is also illustrated by the dramatic overproduction of coccoliths in *E. huxleyi* under nutrient limitation (Balch et al., 1993; Paasche, 1998), and supported by the C_N evidence from *Calcidiscus* and *Helicosphaera* in this study and *Coccolithus* in Gibbs et al., (2013). An alternative possibility is that the continued production of coccoliths by cells in



stationary phase leaves them poised and ‘ready-to-divide’ should nutrients become newly available. The recommencement of cell division in stationary phase cultures after the addition of nutrient-replete seawater has been observed in *E. huxleyi* cultures (J. Young, pers. comms.).

4.2 Contrasting growth phase and growth rate

290 The clear relationship we observe between growth *phase*, Θ and C_N is interpreted to be the result of cellular physiology (calcification, biomass production and the synthesis of molecules involved in cell division) responding to shifts in nutrient availability over the course of the experiments, with stationary-phase nutrient depletion decreasing growth rates to zero once levels became inhibiting to cell division. Exponential-phase growth *rates*, the proportion of the culture undergoing cell division between two consecutive days or averaged across multiple days, are instead affected by temperature, which
295 determines the rate of nutrient uptake and the rate of metabolic cell processes, and irradiance, which affects photosynthetic rates, i.e., the rate at which the cell can produce energy. Our manipulation of experiment temperature (16–22 °C) aimed to achieve a range in exponential-phase growth rates that might reveal any correlation between growth *rate* and coccosphere geometry. However, no clear relationship between Θ , Θ , C_L or C_N and exponential growth rate (daily or mean) was observed in our experiments. One explanation might be that exponential growth rates (μ_{exp}) were not that sensitive to the temperature
300 range we applied (*C. quadripforatus* μ_{exp} =0.30–0.44 d^{−1}; *C. leptoporus* μ_{exp} =0.36–0.44 d^{−1}; *H. carteri* μ_{exp} =0.29–0.44 d^{−1}). In addition, growth rates would not necessarily be expected to influence coccosphere geometry in the same way as a shift in growth phase caused by nutrient depletion, as temperature and light primarily affect physiological rates (e.g., Eppley, 1972; Falkowski et al., 1985) whilst nutrient limitation primarily impedes molecule synthesis (e.g., Zhao et al., 2015). Calcification, for example, is contingent on both the rate at which nutrients can be supplied to the cell (temperature-
305 dependent) and processed into energy (light-dependent) and can proceed under nutrient limitation, as shown in our experiments, but may be less efficient under sub-optimal temperature or light conditions. As yet, no studies have investigated the response of cell size and/or coccosphere geometry under a range of optimum vs. limiting temperature or light conditions in coccolithophores.

4.3 Coccosphere geometry as a proxy for growth phase in the fossil record

310 A notable finding of this study is that coccosphere geometry (coccosphere size, coccolith length and coccoliths per cell) is species-specific but responds identically to growth phase across four different species of *Calcidiscus*, *Coccolithus* and *Helicosphaera*. This strongly suggests that coccosphere geometry within the major coccolithophore families Calcidiscaceae and Helicosphaeraceae responds to nutrient-driven changes in growth phase, and therefore cell physiology, in the same way as species within the families Coccolithaceae (Gibbs et al., 2013) and Noelaerhabdaceae (Balch et al., 1993; Paasche, 1998;
315 Gibbs et al., 2013). This is compelling evidence that, as a group, coccolithophores express a common physiological response to shifts from exponential to non-exponential (stationary) growth phase that is seen as a modest but significant increase in



the average C_N and \emptyset (Fig. 3, 4). This specifically results from the ability of the cell to maintain calcification processes even when rates of cell division are suppressed by nutrient limitation.

One of the aims of this study was to further develop the proxy application of fossil coccosphere geometry that was initially proposed by Gibbs et al. (2013) for *Coccolithus* and *Toweius*. Culture experiments on *Coccolithus* and *Emiliana huxleyi* showed that \emptyset and C_N responded to growth phase as described above and they applied this as a framework for interpreting the coccosphere geometry records of fossil *Coccolithus* and an ancestor of *E. huxleyi* called *Toweius* during the Paleocene-Eocene Thermal Maximum climate change event (56 Ma). Given the tendency of coccolithophores to show strong species- and strain-specific responses to external parameters, applying this framework to other fossil species would be highly speculative based on data from only two modern species. The new experimental data presented here for *Calcidiscus* and *Helicosphaera*, in combination with previous results from *Coccolithus* and *Emiliana* (Balch et al., 1993; Paasche, 1998; Gibbs et al., 2013; Gerech et al., 2014; Gerech et al., 2015), provides validity that coccosphere geometry persistently responds to growth phase in a common manner, regardless of species, and notably that mean population C_N increases under slowed growth in *Calcidiscus*, *Helicosphaera*, *Coccolithus* and *Emiliana*.

To further develop this proxy we need to establish threshold values of C_N that identify recently-divided cells and cells with theoretically sufficient coccoliths to undergo cell division. As an exponential-growth phase population is undergoing cell division at a rapid rate, it has a greater percentage of recently-divided cells ($C_N \leq$ lower threshold; Table 1). In contrast, a slowly-dividing population in stationary-phase growth has a greater percentage of ready-to-divide cells ($C_N \geq$ upper threshold; Table 1) but fewer recently-divided cells. Here, we report these C_N threshold values (Table 1) for *Calcidiscus* and *Helicosphaera* (Fig. 3) and add them to those identified by Gibbs et al. (2013) for *Coccolithus*. C_N is relatively easy to measure in both fossil and modern coccospheres using light microscopy, and so potentially provides a robust method for identifying populations that are growing rapidly (exponential populations where $> \sim 15\%$ population is characterised by cells with C_N typical of recently-divided cells) compared to populations that are growing slowly (non-exponential populations where $> \sim 15\%$ population is characterised by cells with C_N typical of ready-to-divide cells). This is illustrated in Fig. 5 and these specific C_N threshold values can be used to approximate the growth state of any fossil or modern population of *Coccolithus*, *Helicosphaera* or *Calcidiscus* species. In reality, the mixing of populations of different growth states in the fossil record (and open ocean) will result in percentages of recently-divided and ready-to-divide cells for a population frequently lying between the two end-members shown in Fig. 5 (Gibbs et al., 2013). However, where time-series of coccosphere geometry data are available, intervals of changing growth states can be identified as substantial temporal shifts in the proportional percentage of recently-divided to ready-to-divide cells.

For fossil taxa that have no direct modern counterpart, the general characteristics of rapidly growing populations consisting of smaller cells with fewer coccoliths relative to slowly dividing populations can be used as a qualitative indicator of changes in growth phase through time. Based on the species studied here, the typical C_N of recently-divided and ready-to-divide cells can be tentatively proposed for any species (living or extinct) based on the 10th and 90th percentiles of the C_N histogram produced from a compiled taxon-specific dataset of coccosphere geometry. Relative changes in the distribution of



C_N through time within any species can then provide a valuable indication of intervals where species may be experiencing nutrient conditions that are more (shift towards lower C_N , recently-divided geometry) or less (shift towards higher C_N , ready-to-divide geometry) favourable for growth. This can be achieved for any taxon by first compiling a dataset of coccosphere geometry for the focal species and then calculating the 10th and 90th percentiles to estimate taxon-specific C_N thresholds.

355 Growth phase can then be estimated by calculating the percentage of each sample with coccospheres of ready-to-divide and recently-divided C_N before plotting as Fig. 5. We would caution users to be mindful that the full range of coccosphere sizes in a species may not be represented in any particular sample and that, as fossil species are typically morphospecies concepts, the range in C_N observed is likely to incorporate multiple intraspecies morphotypes or ecotypes with similar but subtly varied coccosphere geometries. We therefore recommend that as many samples as is feasible are considered in the full dataset
 360 before calculating C_N thresholds and that the minimum to maximum range in coccosphere geometry parameters (Table 1) within modern species are heeded as an indication of how variable coccosphere geometry can be within even a single clone.

Whilst we conclude that coccosphere geometry can be used with confidence as a proxy of growth phase in the fossil record or modern ocean, we must be clear that the environmental and growth signal recorded in field populations is always more complex than any laboratory experiment results. Populations may only experience a specific nutrient state for a few
 365 weeks or less before conditions change and the coccosphere geometry response of any individual cell to the experienced nutrient state is likely to be further complicated by temperature and light conditions that are also essential for growth. At present there is little to no experimental data to demonstrate the response of coccosphere geometry specifically to temperature or irradiance, or how changes in growth rate specifically (rather than growth phase) driven by these conditions may manifest in coccosphere geometry. The fossil record of coccosphere geometry further compounds these considerations,
 370 as fossil assemblages are typically temporal integrations of many thousands of very short-lived population states. The coccosphere geometry signal of species populations transitioning between rapid and slowed growth phases as nutrient conditions change through time clearly becomes obscured and diluted by the mixing of population remains and subtle shifts in species morphotypes and ecotypes as environmental conditions vary, as illustrated by Gibbs et al. (2013).

Nevertheless, the use of coccosphere geometry as a proxy for growth phase is valid across coccolithophores
 375 generally, and not just specific species. As exponential- and stationary-growth phases describe two distinct physiological states, the former with rapid growth rates experiencing optimal nutrient supply and the latter with slowed growth rates suffering nutrient limitation, coccosphere geometry provides a unique link between the physiology of individual cells, population fitness (measured as growth rate) and ultimately the long-term success of species responding to varying nutrient conditions. As such, the coccosphere geometry-growth phase proxy is a highly valuable tool for evolutionary and
 380 palaeoceanographic studies.

4.4 Implications of growth-driven cellular PIC and POC for calcite production

Coccolithus, *Calcidiscus* and *Helicosphaera* are potentially major regional calcite producers in both the modern (Daniels et al., 2014; Daniels et al., 2016) and past ocean (Ziveri et al., 2007), as they are some of the largest, most heavily calcified



modern species with distributions throughout sub-Polar (*C. pelagicus*), temperate (*C. braarudii*), and sub-tropical
385 (*Calcidiscus* and *Helicosphaera*) oceans (Ziveri et al., 2004). The process of biogenic calcification is thought to be
responsive to climate and particularly sensitive to changes in ocean carbonate chemistry (for reviews see Riebesell and
Tortell, 2011; Bach et al., 2015; Meyer and Riebesell, 2015). Our experiments show that calcite per cell can change
significantly with growth phase by means of variability in the number of coccoliths in the coccosphere as cellular physiology
responds to changing nutrient availability. This was not known for any species other than *E. huxleyi*, which produces high
390 C_N , multi-layered coccospheres under nutrient limitation. *E. huxleyi* additionally sheds excess coccoliths into the surrounding
waters (Balch et al., 1993), potentially amplifying the biogeochemical impact of increased coccolith production under low
nutrient conditions, although, to our knowledge, this species is unique in this respect. Calcite production is a function of
cellular calcite (particulate inorganic carbon, PIC) and growth rate, and could therefore change considerably with
environmental conditions through time with implications for the biogeochemical cycling of carbon in the ocean.

395 PIC can be calculated directly from the extensive dataset of coccosphere geometry collated for this study. This is
achieved by multiplying C_N by coccolith calcite, following Eq. (1) (Sect. 2.4; Young and Ziveri, 2000). Mean cellular PIC
averaged across exponential growth phase days is 11-15 pmol C cell⁻¹ in *C. leptoporus* and 16-18 pmol C cell⁻¹ in *H. carteri*,
but higher in *C. quadriperforatus* and *C. braarudii* at ~30 pmol C cell⁻¹ (Fig. 6). Mean PIC increases during non-exponential
experiment days in all species due to an average increase of 2-4 coccoliths per cell (Fig. 3). The 25th and 75th percentiles are
400 also clearly shifted towards higher cellular PIC in cells no longer growing exponentially (Fig. 6a.). *Calcidiscus* 25th
percentile increases 50-60%, with *C. braarudii* and *H. carteri* increasing 20-25%. The increase in 75th percentile is not as
large but is still considerable in *C. leptoporus* and *C. braarudii* at 36% and 24%, respectively, with *C. quadriperforatus* and
H. carteri showing more modest increases of 6% and 11%.

Calcite production per cell per day is calculated by multiplying cellular calcite by growth rate. Calcite production in
405 these four species is 6-20 times higher than in *E. huxleyi* at a comparable growth rate (Fig. 6; Balch et al., 1996; Poulton et
al., 2010), therefore these heavily calcified species (e.g., the calcite of one *C. braarudii* cell is equivalent to ~78 cells of *E.*
huxleyi) do not necessarily need to be abundant or maintain comparative growth rates to dominate calcite production
(Daniels et al., 2014; Daniels et al., 2016). A dramatic difference in calcite production can be seen between populations
growing exponentially and those no longer growing exponentially, with reductions in calcite production of 77-88% in all
410 species due to the approximate order of magnitude decrease in growth rates (Fig. 6c). In field populations, growth rates can
reach as low as <0.2 d⁻¹ (Poulton et al., 2014), similar to the culture populations in slowed growth shown in Fig. 6, and
therefore these shifts to such low calcite production per cell per day are approximate minimum calcite production values for
these species. However, it is clear that rates of calcite production can be altered by up to 50% for even a moderate change of
growth rate of 0.1-0.2 d⁻¹, for example where coccolithophore populations experience changes in nutrient supply,
415 temperature or light that no longer support optimal rates of cell division (Poulton et al., 2014).

The majority of studies attribute the response of calcite production to environmental change to changes in calcite per
coccolith through coccolith size, thickness or malformation (e.g., Beaufort et al., 2011; Horigome et al., 2014). However, C_L



would need to increase by roughly 5-20% to achieve the same change in cellular calcite as that produced by the increase of just 2-4 coccoliths per cell based on our data. O'Dea et al. (2014) similarly found that changes in coccolith calcite mass of
420 ~5-11% and ~6-16% for *Toweius pertusus* and *Coccolithus pelagicus* during the PETM were dwarfed by up to 500% changes in cellular calcite resulting from combined changes in C_L , \emptyset , and C_N across the same interval of Paleogene climate change. Changes in C_N with growth phase are therefore key when considering the impact of environmental parameters such as nutrient availability on cellular PIC and calcite production rates. The dominant control of growth rates on calcite production is an important consideration that is often overlooked when investigating the impact of climate on long-term
425 calcite production, carbon export, and sequestration and should be accounted for alongside growth phase changes in calcite.

5. Conclusions

Experiments on modern species of the coccolithophores *Calcidiscus* and *Helicosphaera* have shown significant differences in coccosphere geometry under exponential-phase growth (nutrient replete conditions) and non-exponential-phase growth (nutrient depleted conditions) identical to those previously observed in *Coccolithus* and *Emiliana huxleyi*. The extension of
430 these previously published findings into two additional families demonstrates that the decoupling of cell division and calcification in coccolithophores is a core physiological response to nutrient depletion revealed in coccosphere geometry as an increase in coccoliths per cell and coccosphere size. With due consideration, coccosphere geometry can now be applied as a proxy for growth phase in the geological record, as well as in sediment trap and modern field population samples, with the expectation that populations of any coccolithophore species experiencing growth-limiting nutrient conditions will have a
435 greater number of larger cells with more coccoliths per cell. The variability of coccosphere geometry with growth, specifically calcite production through the production of coccoliths, identifies coccoliths per cell as an equally important parameter as calcite per coccolith in determining cellular calcite. Growth rate is the principal driver of calcite production rather than cellular calcite, highlighting the need for accessing growth information in both the modern ocean and geological record in order to explore the impact of future climate change scenarios on calcite production and export.

440

445



Data availability

The coccosphere geometry data and accompanying culture conditions generated for this study are publically accessible as Sheward et al. (2016) at <https://doi.pangaea.de/10.1594/PANGAEA.865403>, doi registration in progress.

Author contributions

450 RS, AP and SG conceived the design of the experiment with advice from CD. RS performed the culturing experiments, collected and analysed the data. RS, SG and AP interpreted the findings. RS wrote the manuscript with contributions from all authors.

The authors declare that they have no conflict of interest.

455 Acknowledgements

We would like to thank Ian Probert (Roscoff Culture Collection) for his provision of the coccolithophore cultures used in this study and Lucie Munns for laboratory assistance. We thank Ros Rickaby for her useful discussions on a previous version of this manuscript. RS was funded by a Vice Chancellors Studentship from the University of Southampton and a Natural Environmental Research Council (NERC) award (reference 1272561). We acknowledge research support from NERC (AP
460 NERC National Capability funding and CD via a NERC studentship) and the Royal Society (SG).

465

470

475



References

- Arrigo, K. R.: Marine microorganisms and global nutrient cycles, *Nature*, 437, 349–355, doi:10.1038/nature04159, 2005.
- Bach, L. T., Riebesell, U., Gutowska, M. A., Federwisch, L. and Schulz, K. G.: A unifying concept of coccolithophore sensitivity to changing carbonate chemistry embedded in an ecological framework, *Prog. Oceanogr.*, 135, 125–138, doi:10.1016/j.pocean.2015.04.012, 2015.
- Balch, W. M., Kilpatrick, K. A., Holligan, P. M. and Cucci, T.: Coccolith production and detachment by *Emiliana huxleyi* (Prymnesiophyceae), *J. Phycol.*, 29(5), 566–575, doi: 10.1111/j.0022-3646.1993.00566.x., 1993.
- Balch, W. M., Fritz, J. and Fernandez, E.: Decoupling of calcification and photosynthesis in the coccolithophore *Emiliana huxleyi* under steady-state light-limited growth, *Mar. Ecol. Prog. Ser.*, 142, 87–97, doi:10.3354/meps142087, 1996.
- Baumann, K. –H.: Importance of size measurements for coccolith carbonate flux estimates, *Micropaleontology*, 50(1), 35–43, 2004.
- Baumann, K. –H., Saavedra-Pellitero, M., Böckel, B., and Ott, C.: Morphometry, biogeography and ecology of *Calcidiscus* and *Umbilicosphaera* in the South Atlantic, *Revue de Micropaléontologie*, 59, 239–251, doi: 10.1016/j.revmic.2016.03.001, 2016.
- Beaufort, L., Probert, I., de Garidel-Thoron, T., Bendif, E. M., Ruiz-Pino, D., Metzl, N., Goyet, C., Buchet, N., Coupel, P., Grelaud, M., Rost, B., Rickaby, R. E. M. and de Vargas, C.: Sensitivity of coccolithophores to carbonate chemistry and ocean acidification., *Nature*, 476, 80–3, doi:10.1038/nature10295, 2011.
- Bollmann, J., Baumann, K. –H., Thierstein, H. R.: Calibration of Gephyrocapsa coccolith abundance in Holocene sediments for paleotemperature assessment, *Paleoceanography*, 17, 1–9, 2002.
- Bollmann, J., Herrle, J. O., Cortés, M. Y., and Fielding, S. R.: The effect of sea water salinity on the morphology of *Emiliana huxleyi* in plankton and sediment samples, *Earth Planet. Sc. Lett.*, 284, 320–328, doi: 10.1016/j.epsl.2009.05.003, 2009.
- Bown, P. R.: Palaeogene calcareous nannofossils from the Kilwa and Lindi areas of coastal Tanzania (Tanzania Drilling Project 2003–2004), *J. Nannoplankt. Res.*, 27(1), 21–95, 2005.
- Bown, P. and Pearson, P.: Calcareous plankton evolution and the Paleocene/Eocene thermal maximum event: New evidence from Tanzania, *Mar. Micropaleontol.*, 71(1–2), 60–70, doi:10.1016/j.marmicro.2009.01.005, 2009.
- Bown, P. R., Lees, J. A. and Young, J. R.: Calcareous nannoplankton evolution and diversity through time, in: *Coccolithophores: from molecular processes to global impact*, Thierstein, H. R., and Young, J. R. (Eds.), Springer, Berlin, 481–508, 2004.
- Bown, P. R., Jones, T. D. and Young, J. R.: *Umbilicosphaera jordanii* Bown, 2005 from the Paleogene of Tanzania: confirmation of generic assignment and a Paleocene origination for the Family Calcidiscaceae, *J. Nannoplankt. Res.*, 29(1), 25–30, 2007.
- Bown, P. R., Gibbs, S. J., Sheward, R. and O’Dea, S. A.: Searching for cells: the potential of fossil coccospheres in



- coccolithophore research, J. Nanoplankt. Res., 34, 5–21, 2014.
- 510 Broecker, W. and Clark, E.: Ratio of coccolith CaCO_3 to foraminifera CaCO_3 in late Holocene deep sea sediments, Paleocceanography, 24(3), 1–11, doi:10.1029/2009PA001731, 2009.
- Buitenhuis, E. T., Pangerc, T., Franklin, D. J., Le Quéré, C., and Malin, G.: Growth rates of six coccolithophorid strains as a function of temperature, Limnol. Oceanogr., 53(3), 1181–1185, doi:10.4319/lo.2008.53.3.1181, 2008.
- Candelier, Y., Minoletti, F., Probert, I. and Hermoso, M.: Temperature dependence of oxygen isotope fractionation in
515 coccolith calcite: A culture and core top calibration of the genus *Calcidiscus*, Geochim. Cosmochim. Acta, 100, 264–281, doi:10.1016/j.gca.2012.09.040, 2013.
- Daniels, C. J., Sheward, R. M. and Poulton, A. J.: Biogeochemical implications of comparative growth rates of *Emiliania huxleyi* and *Coccolithus* species, Biogeosciences, 11, 6915–6925, doi:10.5194/bg-11-6915-2014, 2014.
- Daniels, C. J., Poulton, A. J., Young, J. R., Esposito, M., Humphreys, M. P., Ribas-Ribas, M., Tynan, E. and Tyrrell, T.:
520 Species-specific calcite production reveals *Coccolithus pelagicus* as the key calcifier in the Arctic Ocean, Mar. Ecol. Prog. Ser., 555, 29–47, doi:10.3354/meps11820, 2016.
- Eppley, R. W.: Temperature and phytoplankton growth in the sea, Fish. Bull., 70(4), 1063–1085, 1972.
- Falkowski, P. G., Dubinsky, Z. and Wyman, K.: Growth-irradiance relationships in phytoplankton, Limnol. Oceanogr., 30(2), 311–321, 1985.
- 525 Fiorini, S., Gattuso, J. P., van Rijswijk, P. and Middelburg, J.: Coccolithophores lipid and carbon isotope composition and their variability related to changes in seawater carbonate chemistry, J. Exp. Mar. Bio. Ecol., 394(1–2), 74–85, doi:10.1016/j.jembe.2010.07.020, 2010.
- Fiorini, S., Middelburg, J. J. and Gattuso, J.-P.: Testing the effects of elevated $p\text{CO}_2$ on Coccolithophores (Prymnesiophyceae): Comparison between haploid and diploid life stages, J. Phycol., 47, 1281–1291, doi:10.1111/j.1529-
530 8817.2011.01080.x, 2011.
- Geisen, M., Billard, C., Broerse, A. T. C., Cros, L., Probert, I. and Young, J. R.: Life-cycle associations involving pairs of holococcolithophorid species: intraspecific variation or cryptic speciation?, Eur. J. Phycol., 37, 531–550, doi: 10.1017/S0967026202003852, 2002.
- Geisen, M., Young, J. R., Probert, I., Saez, A. G., Baumann, K. H., Sprengel, C., Bollmann, J., Cros, L., de Vargas, C. and
535 Medlin, L. K.: Species level variation in coccolithophores, in: Coccolithophores: from molecular processes to global impact, Thierstein, H. R., and Young, J. R. (Eds.), Springer, Berlin, 327–366, 2004.
- Gerecht, A. C., Šupraha, L., Edvardsen, B., Probert, I. and Henderiks, J.: High temperature decreases the PIC/POC ratio and increases phosphorus requirements in *Coccolithus pelagicus* (Haptophyta), Biogeosciences, 11, 3531–3545, doi:10.5194/bg-11-3531-2014, 2014.
- 540 Gerecht, A. C., Šupraha, L., Edvardsen, B., Langer, G. and Henderiks, J.: Phosphorus availability modifies carbon production in *Coccolithus pelagicus* (Haptophyta), J. Exp. Mar. Bio. Ecol., 472, 24–31, doi:10.1016/j.jembe.2015.06.019, 2015.



- Gibbs, S. J., Bralower, T. J., Bown, P. R., Zachos, J. C. and Bybell, L. M.: Shelf and open-ocean calcareous phytoplankton assemblages across the Paleocene-Eocene Thermal Maximum: Implications for global productivity gradients, *Geology*, 34, 233, doi:10.1130/G22381.1, 2006.
- Gibbs, S. J., Poulton, A. J., Bown, P. R., Daniels, C. J., Hopkins, J., Young, J. R., Jones, H. L., Thiemann, G. J., O'Dea, S. A. and Newsam, C.: Species-specific growth response of coccolithophores to Palaeocene–Eocene environmental change, *Nat. Geosci.*, 6(3), 218–222, doi:10.1038/ngeo1719, 2013.
- Haq, B. U., Lohmann, G. P.: Early Cenozoic calcareous nannoplankton biogeography of the Atlantic Ocean, *Mar. Micropaleontol.*, 1, 119–194, 1976.
- Henderiks, J., and Törner, A.: Reproducibility of coccolith morphometry: Evaluation of spraying and smear slide preparation techniques, *Mar. Micropaleontol.*, 58, 207–218, doi:10.1016/j.marmicro.2005.11.002, 2006.
- Herrmann, S., Weller, A. F., Heneriks, J., and Thierstein, H. R.: Global coccolith size variability in Holocene deep-sea sediments, *Mar. Micropaleontol.*, 82–83, 1–12, doi:10.1016/j.marmicro.2011.09.006, 2012.
- Horigome, M. T., Ziveri, P., Grelaud, M., Baumann, K.-H., Marino, G. and Mortyn, P. G.: Environmental controls on the *Emiliania huxleyi* calcite mass, *Biogeosciences*, 11, 2295–2308, doi:10.5194/bg-11-2295-2014, 2014.
- Janofske, D.: Calcareous nannofossils of the Alpine Upper Triassic, in: *Nannoplankton Research (Proceedings of the INA Conference)*, Hamrsmid, B. and Young, J. R. (Eds.), Knihovnicka ZPN, Hodonin, Czech Republic, 87–109, 1992.
- Knappertsbusch, M.: Morphologic evolution of the coccolithophorid *Calcidiscus leptoporus* from the Early Miocene to recent, *J. Paleontol.*, 74(4), 712–730, 2000.
- Knappertsbusch, M., Cortes, M. Y. and Thierstein, H. R.: Morphologic variability of the coccolithophorid *Calcidiscus leptoporus* in the plankton, surface sediments and from the Early Pleistocene, *Mar. Micropaleontol.*, 30, 293–317, 1997.
- Krug, S. A., Schulz, K. G. and Riebesell, U.: Effects of changes in carbonate chemistry speciation on *Coccolithus braarudii*: A discussion of coccolithophorid sensitivities, *Biogeosciences*, 8, 771–777, doi:10.5194/bg-8-771-2011, 2011.
- Langer, G., Geisen, M., Baumann, K.-H., Kläs, J., Riebesell, U., Thoms, S. and Young, J. R.: Species-specific responses of calcifying algae to changing seawater carbonate chemistry, *Geochemistry, Geophys. Geosystems*, 7(9), Q09006, doi:10.1029/2005GC001227, 2006.
- Langer, G., Nehrke, G., Probert, I., Ly, J. and Ziveri, P.: Strain-specific responses of *Emiliania huxleyi* to changing seawater carbonate chemistry, *Biogeosciences*, 6, 2637–2646, doi:10.5194/bg-6-2637-2009, 2009.
- Langer, G., Oetjen, K. and Brenneis, T.: Calcification of *Calcidiscus leptoporus* under nitrogen and phosphorus limitation, *J. Exp. Mar. Bio. Ecol.*, 413, 131–137, doi:10.1016/j.jembe.2011.11.028, 2012.
- Menden-Deuer, S. and Kiørboe, T.: Small bugs with a big impact: linking plankton ecology with ecosystem processes, *J. Plankton Res.*, 38 (4), 1036–1043, doi:10.1093/plankt/fbw049, 2016.
- Meyer, J. and Riebesell, U.: Reviews and Syntheses: Responses of coccolithophores to ocean acidification: a meta-analysis, *Biogeosciences*, 12, 1671–1682, doi:10.5194/bg-12-1671-2015, 2015.



- Monteiro, F. M., Bach, L. T., Brownlee, C., Bown, P., Rickaby, R. E. M., Poulton, A. J., Tyrrell, T., Beaufort, L., Dutkiewicz, S., Gibbs, S., Gutowska, M. A. and Lee, R.: Why marine phytoplankton calcify, *Sci. Adv.*, 2, e1501822, doi: 10.1126/sciadv.1501822, 2016.
- Moore, C. M., Mills, M. M., Arrigo, K. K., Berman-Frank, I., Bopp, L., Boyd, P. W., Galbraith, E. D., Geider, R. J., Guieu, C., Jaccard, S. L., Jickells, T. D., La Roche, J., Lenton, T. M., Mahowald, N. M., Marañón, E., Marinov, I., Moore, J. K., Nakatsuka, T., Oschlies, A., Saito, M. A., Thingstad, T. F., Tsuda, A. and Ulloa, O.: Processes and patterns of nutrient limitation, *Nat. Geosci.*, 6, 701–710, doi:10.1038/NGEO1765, 2013.
- Müller, M. N., Antia, A. N. and La Roche, J.: Influence of cell cycle phase on calcification in the coccolithophore *Emiliania huxleyi*, *Limnol. Oceanogr.*, 53(2), 506–512, 2008.
- Müller, M. N., Lebrato, M., Riebesell, U., Barcelos e Ramos, J., Schulz, K. G., Blanco-Ameijeiras, S., Sett, S., Eisenhauer, A. and Stoll, H. M.: Influence of temperature and CO₂ on the strontium and magnesium composition of coccolithophore calcite, *Biogeosciences*, 11, 1065–1075, doi:10.5194/bg-11-1065-2014, 2014.
- O’Dea, S. A., Gibbs, S. J., Bown, P. R., Young, J. R., Poulton, A. J., Newsam, C. and Wilson, P. A.: Coccolithophore calcification response to past ocean acidification and climate change, *Nat Commun.*, 5, 5363, doi: 10.1038/ncomms6363, 2014.
- Paasche, E.: Roles of nitrogen and phosphorus in coccolith formation in *Emiliania huxleyi* (Prymnesiophyceae), *Eur. J. Phycol.*, 33, 33–42, doi:10.1017/S0967026297001480, 1998.
- Perch-Nielsen, K.: Cenozoic calcareous nannofossils, in: *Plankton Stratigraphy*, Bolli, H. M., Saunders, J. B. and Perch-Nielsen, K. (Eds.), Cambridge University Press, Cambridge, 427–555, 1985.
- Poulton, A. J., Charalampopoulou, A., Young, J. R., Tarran, G. A., Lucas, M. I. and Quartly, G. D.: Coccolithophore dynamics in non-bloom conditions during late summer in the central Iceland Basin (July–August 2007), *Limnol. Oceanogr.*, 55(4), 1601–1613, doi:10.4319/lo.2010.55.4.1601, 2010.
- Poulton, A. J., Stinchcombe, M. C., Achterberg, E. P., Bakker, D. C. E., Dumousseaud, C., Lawson, H. E., Lee, G. A., Richier, S., Suggett, D. J. and Young, J. R.: Coccolithophores on the north-west European shelf: Calcification rates and environmental controls, *Biogeosciences*, 11, 3919–3940, doi:10.5194/bg-11-3919-2014, 2014.
- Renaud, S., Ziveri, P. and Broerse, A. T. C.: Geographical and seasonal differences in morphology and dynamics of the coccolithophore *Calcidiscus leptoporus*, *Mar. Micropaleontol.*, 46, 363–385, doi: 10.1016/S0377-8398(02)00081-6, 2002.
- Riebesell, U. and Tortell, P. D.: Effects of ocean acidification on pelagic organisms and ecosystems, in: *Ocean Acidification*, Gattuso, J.-P. and Hansson, L. (Eds.), Oxford University Press, Oxford, 99–121, 2011.
- Sáez, A. G., Probert, I., Geisen, M., Quinn, P., Young, J. R. and Medlin, L. K.: Pseudo-cryptic speciation in coccolithophores., *Proc. Natl. Acad. Sci. USA.*, 100(12), 7163–8, doi:10.1073/pnas.1132069100, 2003.
- Sheward, R. M., Daniels, C. J. and Gibbs, S. J.: Growth rates and biometric measurements of coccolithophores (*Coccolithus pelagicus*, *Coccolithus braarudii*, *Emiliania huxleyi*) during experiments, doi:10.1594/PANGAEA.836841, 2014.
- Sheward, R. M., Poulton, A. J. and Gibbs, S. J.: Cocosphere geometry measurements from culture experiments on the



- 610 coccolithophore species *Calcidiscus leptoporus*, *Calcidiscus quadriperforatus* and *Helicosphaera carteri*, doi registration pending, 2016.
Stoll, H. M., Klaas, C. M., Probert, I., Encinar, J. R. and Alonso, J. I. G.: Calcification rate and temperature effects on Sr partitioning in coccoliths of multiple species of coccolithophorids in culture, *Glob. Planet. Change*, 34(3–4), 153–171, doi:10.1016/S0921-8181(02)00112-1, 2002.
- 615 Sun, J. and Liu, D.: Geometric models for calculating cell biovolume and surface area for phytoplankton, *J. Plankton Res.*, 25(11), 1331–1346, doi:10.1093/plankt/fbg096, 2003.
Šupraha, L., Gerecht, A. C., Probert, I. and Henderiks, J.: Eco-physiological adaptation shapes the response of calcifying algae to nutrient limitation, *Sci. Rep.*, 5, 16499, doi:10.1038/srep16499, 2015.
Taylor, A. R., Russell, M. A., Harper, G. M., Collins, T. F. T. and Brownlee, C.: Dynamics of formation and secretion of
620 heterococcoliths by *Coccolithus pelagicus* ssp. *braarudii*, *Eur. J. Phycol.*, 42(2), 125–136, doi:10.1080/09670260601159346, 2007.
de Vargas, C., Aubry, M.-P., Probert, I. and Young, J.: Origin and evolution of coccolithophores: From coastal hunters to oceanic farmers, in: *Evolution of Primary Producers in the Sea*, Falkowski, P. G. and Knoll, A. H. (Eds.), Academic Press, San Diego, 251–286, 2007.
- 625 Young, J., Geisen, M., Cros, L., Kleijne, A., Sprengel, C., Probert, I. and Ostergaard, J.: A guide to extant coccolithophore taxonomy, *J. Nannoplankt. Res.*, Special Issue, 2003.
Young, J. R. and Ziveri, P.: Calculation of coccolith volume and its use in calibration of carbonate flux estimates, *Deep Sea Res. Part II Top. Stud. Oceanogr.*, 47, 1679–1700, doi:10.1016/S0967-0645(00)00003-5, 2000.
Zhao, Y., Wang, Y. and Quigg, A.: Comparison of population growth and photosynthetic apparatus changes in response to
630 different nutrient status in a diatom and a coccolithophore, *J. Phycol.*, 51(5), 872–884, doi:10.1111/jpy.12327, 2015.
Ziveri, P., Baumann, K. H., Böckel, B., Bollmann, J. and Young, J. R.: Biogeography of selected Holocene coccoliths in the Atlantic Ocean, in: *Coccolithophores from Molecular Process to Global Impact*, Thierstein, H.R. and Young, J.R. (Eds.), Springer-Verlag, Heidelberg, 403–428, 2004.
Ziveri, P., de Bernardi, B., Baumann, K. H., Stoll, H. M. and Mortyn, P. G.: Sinking of coccolith carbonate and potential
635 contribution to organic carbon ballasting in the deep ocean, *Deep. Res. Part II Top. Stud. Oceanogr.*, 54, 659–675, doi:10.1016/j.dsr2.2007.01.006, 2007.



Tables

645 **Table 1.** Species-specific coccosphere geometry data, PIC (particulate inorganic carbon), POC (particulate organic carbon) and C_N (number of coccoliths per cell) thresholds for classifying the proportion of recently- and ready-to-divide cells in a population.

Parameter		<i>Helicosphaera carteri</i>	<i>Calcidiscus leptoporus</i>	<i>Calcidiscus quadriperforatus</i>	<i>Coccolithus pelagicus</i>	<i>Coccolithus braarudii</i>
Coccosphere diameter, Ø µm	Min	9.35	10.02	13.84	11.74	13.66
	Mean	15.01	13.28	18.56	16.12	20.49
	Max	20.90	19.72	24.39	20.80	29.68
Cell diameter, Ø µm	Min	6.53	6.39	8.64	7.94	9.92
	Mean	12.01	9.90	13.72	12.89	16.36
	Max	17.99	16.54	18.81	18.11	25.83
Coccolith length, C_L µm	Min	6.70	5.02	3.67	5.68	7.87
	Mean	8.89	6.72	8.12	8.95	12.21
	Max	11.22	8.76	11.67	11.59	17.32
Coccoliths per cell, C_N µm	Min	6	10	8	7	5
	Mean	16	19	18	14	12
	Max	30	45	29	23	21
PIC pmol C cell ⁻¹	Min	7.79	3.27	6.09	2.16	4.15
	Mean	24.48	13.00	30.69	17.28	43.62
	Max	54.95	36.58	80.19	211.3	42.08
POC pmol C cell ⁻¹	Min	1.94	1.82	4.27	6.29	3.36
	Mean	11.21	6.57	16.26	13.78	27.77
	Max	33.64	26.55	38.13	93.19	34.27
Recently divided cells $C_N \leq$		$C_N \leq 12$	$C_N \leq 14$	$C_N \leq 14$	$C_N \leq 11$	$C_N \leq 8$
Ready to divide cells $C_N \geq$		$C_N \geq 21$	$C_N \geq 23$	$C_N \geq 25$	$C_N \geq 18$	$C_N \geq 16$
Reference		This study	This study	This study	Sheward et al. (2014)	Gibbs et al. (2013); Sheward et al. (2014)

650



Figures

655

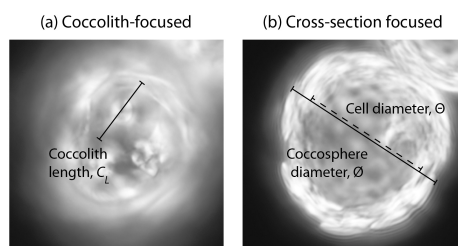


Figure 1. Light microscope image of a *C. quadriperforatus* coccosphere illustrating the coccosphere geometry terminology used in this study and the size measurements made on each individual coccosphere. After counting the number of coccoliths per cell (C_N), images are taken of (a) an in-focus, representative coccolith on either the top or bottom surface of the coccosphere from which coccolith length (C_L) is measured, and (b) a cross-sectional view from which the coccosphere diameter (\emptyset) and internal coccosphere diameter, representing cell diameter (Θ), are measured.

660

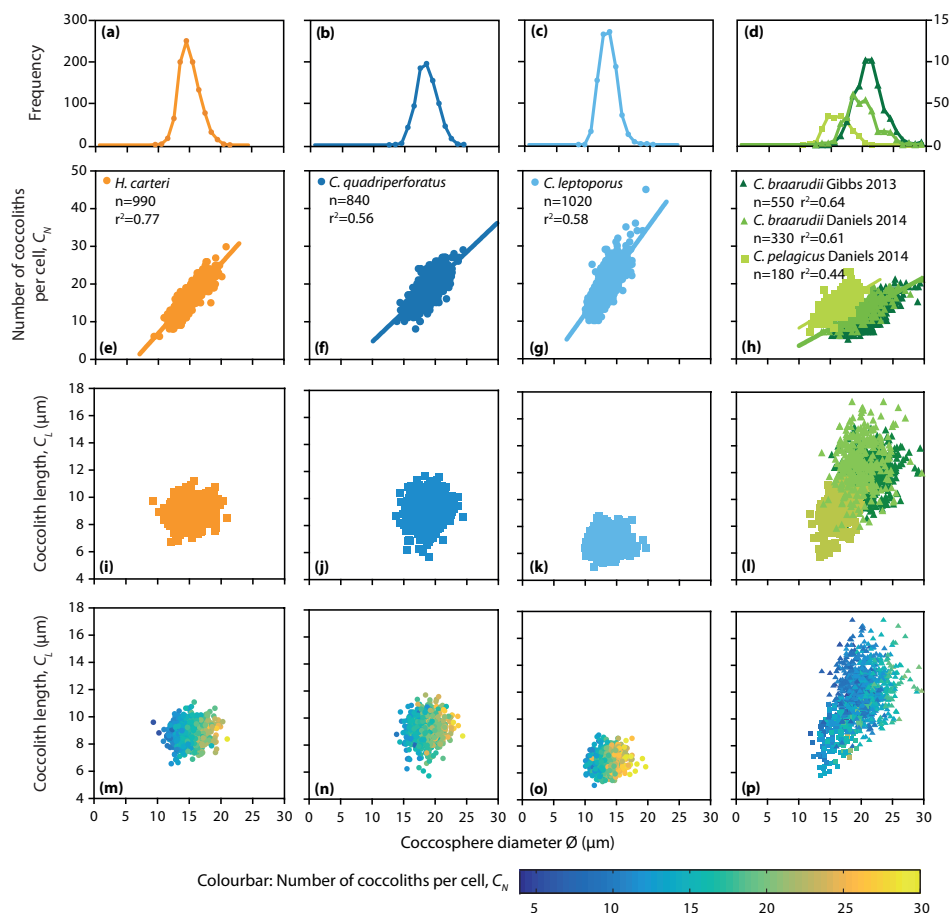


Figure 2. The full range of coccosphere geometry in *H. carteri*, *C. quadriperforatus* and *C. leptoporus*. (a)–(d) Histograms of coccosphere diameter (\emptyset) calculated for frequency bins of $1\mu\text{m}$ size. Note the different frequency scale in plot (d). (e)–(h) Number of coccoliths per cell (C_N) against \emptyset showing a strong and statistically significant ($p<0.0001$) positive relationship. (i)–(l) Coccolith length (C_L) with \emptyset . (m)–(p) C_L and \emptyset with data points coloured by C_N . For comparison purposes, we include data for *C. braarudii* and *C. pelagicus* that can be found in Gibbs et al. (2013) and Sheward et al. (2014) accompanying Daniels et al. (2014).

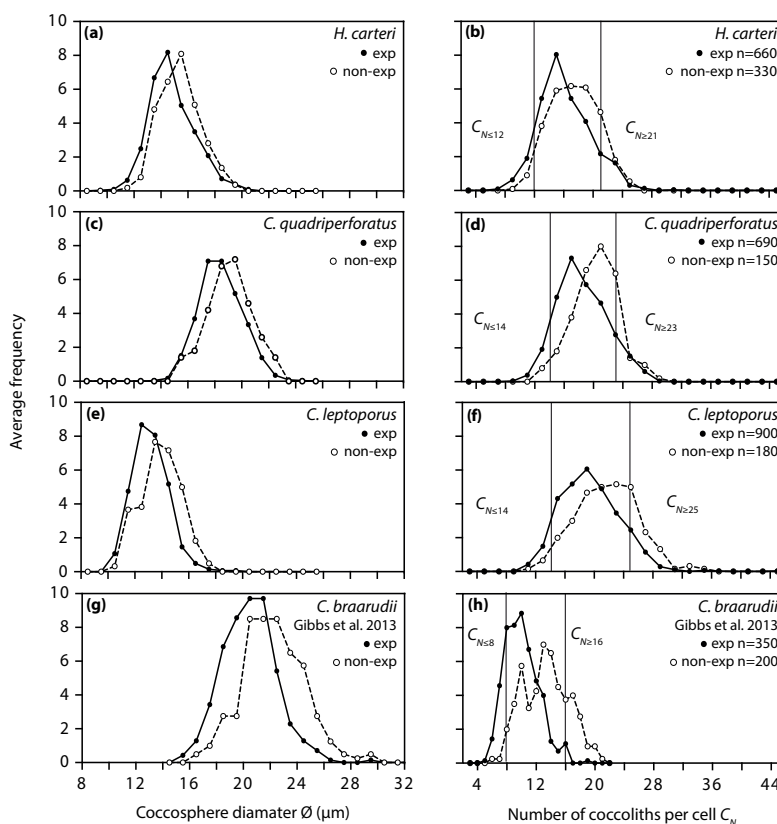
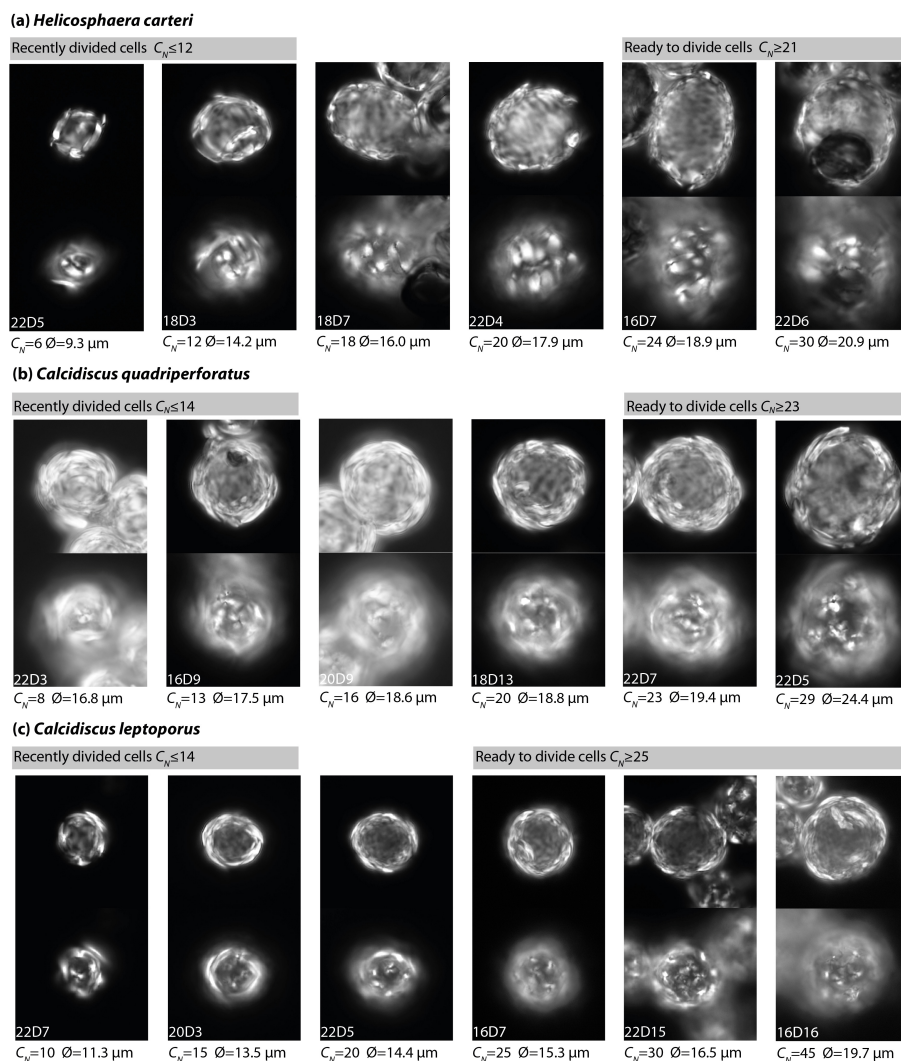


Figure 3. Frequency of coccosphere diameter (\emptyset) and number of cocoliths per cell (C_N) for experiment days in exponential growth (solid line) and experiment days no longer in exponential growth (dashed line), averaged across all temperature treatments. (a)–(f) *H. carteri*, *C. quadriperforatus*, and *C. leptoporus* data from this study. (g)–(h) is a reproduction of *C. braarudii* experiment data from Gibbs et al. (2013) SI Figure 1e. and 1.f for comparison purposes. The lines drawn on C_N plots indicate cells that are recently divided and ready-to-divide/non-dividing, based on the 10th and 90th percentiles of the complete species C_N data shown in Fig. 2.



685 **Figure 4.** Light microscopy images illustrating the range of cell geometry observed within cultures of (a) *H. carteri*, (b) *C.*
quadriperforatus, and (c) *C. leptoporus* at 16–22 °C. The upper image of each pair shows the cross-sectional view of the cell from which
 coccosphere diameter and cell diameter are measured. The lower image of each pair shows a coccolith-focused view of the cell from
 which coccolith length is measured. Number of coccoliths per cell (C_N) and coccosphere diameter (Ø) are given for each cell. A reference
 code for the experiment day that the image was taken from is also given. 22D7 would be a cell from Day 7 of the 22 °C experiment as an
 690 example. All images are to the same scale.

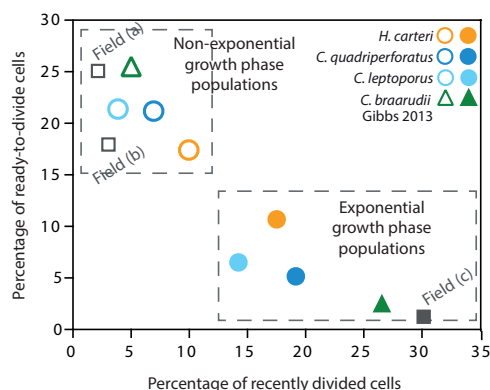
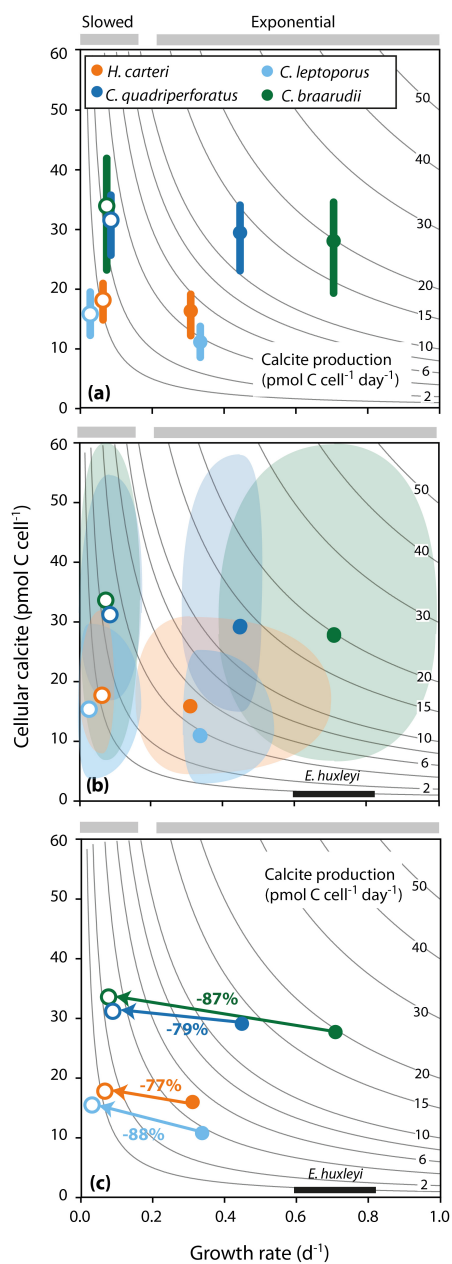


Figure 5. Contrasting exponential and non-exponential phase culture populations based on the percentage of recently divided and ready-to-divide cells within the population, as characterised by C_N thresholds specific to each species (Fig. 3; Table 1). Mean percentages for exponential days are shown as filled data points and the mean non-exponential experiment day percentages are shown as unfilled data points. Also indicated (grey squares) are the characteristic percentages of three *Coccinellithus* field population datasets presented in Gibbs et al. (2013) - Field (a) is Scotland, Field (b) is Iceland non-bloom (both experiencing slowed growth), and Field (c) is Iceland bloom experiencing rapid growth.





720 **Figure 6.** Calcification rates in *Coccolithus*, *Calcidiscus* and *Helicosphaera* at 22 °C. (a) mean and 25th to 75th percentile of cellular calcite for cultures dividing exponentially (filled circles) and cultures no longer maintaining exponential growth (unfilled circles). (b) Range in cellular calcite, growth rates and calcite production observed across the experiment. (c) Percentage decrease in mean calcite production when cultures can no longer divide exponentially. The black box in (b) and (c) represents typical calcite production rates ($\sim 0.2\text{--}0.8$ pmol C cell⁻¹ day⁻¹) for *E. huxleyi* for comparison (Balch et al., 1996, Poulton et al., 2010).